ELSEVIER

Polymer 42 (2001) 9469–9479

polymer

www.elsevier.com/locate/polymer

Polyurethane–unsaturated polyester interpenetrating polymer networks: thermal and dynamic mechanical thermal behaviour

X. Ramis, A. Cadenato, J.M. Morancho, J.M. Salla*

Laboratori de Termodinàmica de la ETSEIB, Universitat Politècnica de Catalunya, Diagonal 647, Barcelona 08028, Spain

Received 22 January 2001; accepted 2 July 2001

Abstract

A series of simultaneous interpenetrating polymer networks, IPNs, based on a polyurethane and an unsaturated polyester resin is studied. The curing process was followed using differential scanning calorimetry (DSC) and Fourier-transform infrared spectroscopy (FTIR). The IPNs were seen to crosslink completely and the kinetics of the curing process were modified greatly, accelerating with respect to the pure homopolymers. The process of styrene–polyester copolymerization varies from an azeotropic copolymerization in the pure polyester state to alternating copolymerization in the IPNs. Miscibility, phase continuity and phase separation are studied by dynamic mechanical thermal analysis (DMTA). In general, the IPNs obtained have a high degree of interpenetration and are semi-miscibles. Intermediate compositions are slightly less miscible than the outer ranges with a transition for the second component being apparent. The empirical loss modulus–composition curves are compared with those predicted by various theoretical models. In general, the IPNs follow the Budiansky model, which predicts a phase inversion at intermediate compositions. Compositions which are rich in a specific component show a continuous phase with the disperse minority component and the intermediate compositions show two co-continuous phases. It is also seen that these curves depend strongly on the temperature at which they are formed. The loss factor reveals strong synergism and the maximum of properties are found in a composition close to 40% in polyester. Comparison of simultaneous IPNs with sequential IPNs showed that the latter show a lesser tendency to phase separation in the systems studied.

Keywords: Interpenetrating polymer networks; Polyurethane; Unsaturated polyester resin

1. Introduction

An interpenetrating polymer network (IPN) may be defined as a mixture of two or more crosslinked polymers in which at least one has been synthesized or crosslinked in the presence of the other. In the ideal case, these materials show a homogenous, isotropic morphology without covalent bonds and with only physical entanglements produced by a partial or total interpenetration between the different networks [1,2].

IPNs may be synthesized sequentially (SEQ-IPN) and simultaneously (SIM-IPN). In sequential synthesis, the first network formed may restrict the formation of the second and limit the range of compositions and properties of the IPNs obtained by this synthetic route. One or more components may not react completely or adequately. In general, simultaneous IPNs show a higher degree of intermixing than sequential IPNs, although in this study, as is discussed below, the reverse was found. Furthermore, in general, compatibility is greater in a mixture of monomers or prepolymers than in a mixture of polymers. The existence of chemical bonding between the two components of the IPN usually produces materials with a greater degree of intermixing [2–4].

The morphology of IPNs tends to be complicated, as there are two competing processes that may take place simultaneously during polymerization: on the one hand, the phase separation of the polymer chains formed, which occurs through diffusion in a medium with increasing viscosity and, on the other, the formation of networks that restrict diffusion. The physical phenomena of gelling (viscosity becomes infinite) and vitrification, along with topological impediments, have an important effect on diffusion and, therefore, on phase separation. Generally, phase separation occurs during polymerization, although in extremely compatible polymers the phase domain size is small. When compatibility decreases, two phases appear with domains of a different structure and size. Normally, when the crosslink density of the polymer that crosslinks first increases, the size of the domains of the polymer that forms second decreases. This effect is reasonable, as the

---

* Corresponding author. Tel.: +34-93-401-6591; fax: +34-93-401-7389.
E-mail address: salla@mmt.upc.es (J.M. Salla).

0032-3861/01/$ - see front matter
PII: S0032-3861(01)00492-X

network initially formed must restrict the size of the regions in which the second polymer may form a separate phase. IPN composition determines the relative amounts of the two phases present after polymerization. When the amount of the second polymer is increased, its domain size generally increases, although this effect will depend on the polymerization method.

From the above it may be said that the morphology and the appearance, to a greater or lesser degree, of phase separation in IPNs fundamentally depends on: the miscibility of the monomers and polymers, IPN composition, crosslinking density in the polymers, the degree of crosslinking reached, inter-network-grafting, reaction conditions (such as temperature and viscosity of the mixture and components) and the relative polymerization rates [2,5].

The most common method of studying miscibility in polymer blends and IPNs is the macroscopic determination of the temperature of the glass transition (or transitions). Completely miscible polymers show a single glass transition between the T_gs of the homopolymers with a similar sharpness to that of the pure components. Partially miscible polymers may show one broad glass transition or two sharp transitions that shift according to the composition. The first case indicates microheterogeneity, in which there are an infinite number of phases of a different composition. In the second case, each phase contains a certain amount of the other component, which shifts the glass transition. When there is clear immiscibility between polymers, two separate glass transitions are seen which are the same as those of the homopolymers. Electron microscopy is usually employed to observe the morphology of these materials. The main difficulty lies in establishing what domain size or different composition phase is needed to be able to see a different macroscopic property (for example, T_g) characteristic of this domain. In some blends, microscopic evidence of phase separation in materials with a single well-defined T_g have been detected. Nevertheless, the existence of one or two glass transitions, their sharpness and positions in blends and IPNs gives an indication of a characteristic macroscopic property of the material and provides a qualitative means of gaining information on miscibility. The observation of a measurable change in the glass transition of an IPN with respect to the pure components is indicative of a high degree of interpenetration [6,7].

Although different families of IPNs have been thoroughly studied, the so-called full-IPNs formed by two crosslinking polymers through a different curing process have, in general, not been extensively studied. In the literature, it is seen that combining crosslinked polymers in different compositions produces IPNs of different morphologies and in some cases, there is a synergistic improvement of properties, which indicates a high degree of interpenetration [2]. For example, the combination of a glassy polymer with a rubbery polymer enables a family of IPNs to be obtained with a wide range of properties, which depend on the component that forms the continuous matrix. These IPNs show properties that range from reinforced rubber, if the elastomer phase is both continuous and dominant, to rubber reinforced high-impact plastics if the glassy phase is continuous [8–14]. In certain polyester–polyurethane IPNs [15] and in polymetacrylate–polyurethane [12,13], an improvement has been noted in some of the following properties produced (synergism): tensile strength, elongation at break, toughness index, impact strength and mechanical damping (tan δ).

There is increasing interest in the use of IPNs in reactive processes such as reaction injection moulding (RIM) [14–19]. The addition of a second reactive phase may improve the properties that are lacking in conventional RIM materials such as polyurethanes (PU). Specifically, the addition of unsaturated polyester (PE) may be considered as an internal reinforcement and may be an interesting alternative to an external reinforcement with glass fibre added to the polyol or to the isocyanate during the RIM process.

In the present study, a family of simultaneous IPNs based on unsaturated polyester and polyurethane resins has been studied. A broad study of this family of IPNs has been attempted which takes in the morphology, the physical properties of the final products and features of the process.

The curing process was followed using differential scanning calorimetry (DSC) and by Fourier-transform infrared spectroscopy (FTIR) spectroscopy with a temperature control unit. Thermomechanical properties of the synthesized IPNs were analysed using a Dynamic Mechanical Thermal Analyser (DMTA). The reaction heats obtained by DSC and analysis of evolution of the glass transition provide knowledge of the extent of the curing process and the thermal characteristics of the IPNs formed and of the starting ingredients prior to crosslinking. The evolution of IR bands associated with the isocyanate and vinyl (unsaturated polyester and styrene) functional groups allows the detailed study of the curing process and determination of the reaction rates of all the reaction groups and confirms the results found by DSC. The DMTA study of the relaxation associated with the glassy transition of the two components of the IPN, the patterns of the extent of the phase separation and the characteristics of the interpenetration reached as a function of the components were deduced. To establish the relative heterogeneity of the IPNs, the elastic moduli obtained by DMTA, were compared with those calculated from modulus–composition theories which predict dual-phase continuity and phase inversion [11–13].

2. Experimental

2.1. Materials

The polyester–polyurethane IPNs studied in this work contain two reactive parts (the polyurethane phase and the polyester phase) designated as IPN*x*PE*y*PU (*x* stands for the % weight of polyester and *y* the % weight of polyurethane).

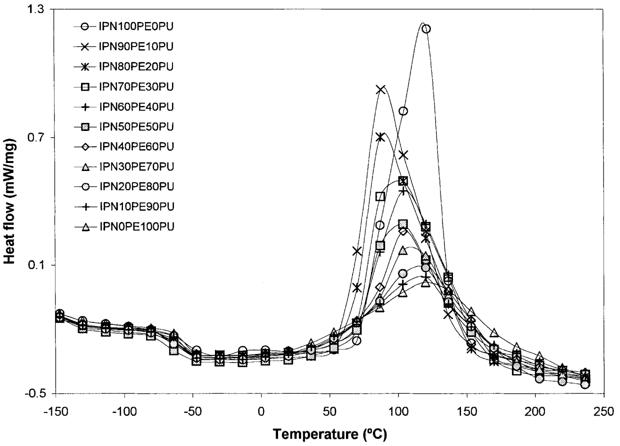

Fig. 1. Dynamic DSC thermogram for IPNs samples cured at 10 K/min.

The polyester phase consists of a resin formed by phthalic anhydride, maleic anhydride and propylene glycol in a molar proportion of 2:1:3, determined by 1H-NMR (Cray Valley A228). The number-average molecular weight is 1696 and the equivalent by mole of C=C is $M = 259$. The resin contains 35% styrene as a crosslinking agent (styrene/unsaturated polyester double bonds molar ratio $S/E = 1.34$) and 50 ppm of hydroquinone as an inhibitor, which was not eliminated. The PE resin had a viscosity of 3.2 poise (25°C). In order to obtain simultaneous IPNs, a solution of 50% methyl ethyl ketone peroxide (MEKP) in dimethyl phthalate (AKZO, Butanox M-50) was used as an initiator and cobalt octoate (CoOc) in a 6% solution of cobalt in dybutyl phthalate (AKZO, Acelerator NL51P) as a promotor of the polyester phase. The ratio between the polyester mass, the initiator and the promotor used was 100:1:0.05. The polyurethane phase is formed by diphenyl-methane-4,4′-diisocyanate (MDI, BASF, Lupranat M20A) with a functionality of $f = 2.7$ and $M = 132.5$ and polypropylenglycol (BASF, Lupranol 1200) with $f = 2$, $M = 224.4$ and an OH index of 250 mg KOH/g. The viscosities (25°C) of the MDI and the polypropylenglycol were 1.8 and 3.25 poise. Before the polyol and the MDI were mixed, they were degassed at 50°C in a vacuum for two hours to eliminate dissolved water and air.

2.2. Differential scanning calorimetry

Calorimetric tests were done on a DSC-30 calorimeter coupled to a Mettler–Toledo TA4000 thermoanalyser. To obtain the glass transition phase temperature, T_{go}, of the uncrosslinked IPNs, the heat of reaction, Δh_{dyn}, and the glass transition temperature of the completely cured material, $T_{g\infty}$, the IPNs were cured from −150 to 250°C at a heating rate of 10 K/min and a second heating was carried out under the same conditions. All of the samples weighed 10 ± 0.2 mg.

2.3. Dynamic mechanical thermal analysis

The DMTA analysis was carried out on a Rheometrics PL-DMTA MK3 analyser. The tests were done from −50 to 200°C at a frequency of 1 Hz and a heating rate of 2 K/min. Single cantilever bending was performed on rectangular samples (5 cm × 12 cm × 1.5 cm). The samples were obtained by curing the IPNs at 60°C for 24 h and then post-curing them for 1 h at 180°C in an oven. Before the samples were made, they were degassed in a vacuum oven until they had nearly gelled.

2.4. FTIR spectroscopy

The curing process was followed using a FTIR Bomem Michelson MB100 spectrophotometer with a resolution of 4 cm^{-1} in the absorbance mode. The uncrosslinked IPNs were placed between two NaCl plates for liquids. The liquid cell was introduced in the oven and this was placed in the FTIR spectrophotometer. The oven was always maintained at 60°C and FTIR spectrum measurements were taken over time. The IPNs reacted under the same conditions as the samples used for the DMTA analysis. The consumption of reactive groups in the polyurethane phase was followed by the changes in absorbance that the band underwent at 2274 cm^{-1} (isocyanate group) [16]. The consumption of C=C in the polyester phase was evaluated by measuring the changes in absorbance at 1645 cm^{-1} (stretching modes of the C=C in polyester) and at 1630 cm^{-1} (stretching modes of vinyl group in styrene) [20,21]. To avoid errors arising from changes in thickness, the 700 cm^{-1} (C–H out-of-plane bending in benzene ring of styrene) [22] band was chosen as an internal standard, as it is practically constant throughout the reaction process. The constancy of this band and the fact that weight losses were not detected indicates that there was no appreciable evaporation of styrene. The absorbencies were calculated as the areas of the peaks. Conversion of the different reactive groups were determined by the Lambert–Beer law from the normalized changes of absorbance as:

$$\alpha = \frac{\dfrac{A_x^0}{A_{700}^0} - \dfrac{A_x^t}{A_{700}^t}}{\dfrac{A_x^0}{A_{700}^0}} \tag{1}$$

where A_x^0 and A_x^t are the initial absorbencies and at a time t for polyester, styrene or the isocyanate at $x = 1645$, 1630 or 2274 cm^{-1}. A_{700}^0 and A_{700}^t are the initial absorbencies and at time t at 700 cm^{-1}. The total conversion of C=C double bonds in the unsaturated polyester resin was determined as:

$$\alpha_T = \frac{(S/E)\alpha_S + \alpha_E}{1 + (S/E)} \tag{2}$$

where α_S and α_E are the conversions of the styrene and polyester C=C bonds and (S/E), which has a value of

Table 1

Results of the DSC and DMTA analysis for the polyurethane–polyester IPNs studied (Δh_{dyn}: experimental reaction heat; Δh_{theo}: theoretical reaction heat; T_{p}: temperature of the calorimetric peak; T_{go}: temperature of calorimetric glass transition of material without crosslinking; $T_{\mathrm{g}\infty}$: temperature of calorimetric glass transition of completely reacted material. E_{r}: equilibrium modulus of material in the rubbery region; d: density; M_{c}: number-average molecular weight between crosslinks; T_1 and T_2: maximum temperatures of tan δ; $T_{E''}$: maximum temperature of E'')

	DSC					DMTA					
IPN	Δh_{dyn} (J/g)	Δh_{theo} (J/g)	T_{p} (°C)	T_{go} (°C)	$T_{\mathrm{g}\infty}$ (°C)	E_{r} (MPa)	d (g/cm^3)	M_{c}	T_1 (°C)	T_2 (°C)	$T_{E''}$(°C)
IPN100PE0PU	384.1	384.1	121	− 59	101	61.24	1.17	220.0		139	109
IPN90PE10PU	365.3	365.9	89	− 59	93	36.20	1.16	361.6		129	80
IPN80PE20PU	347.1	347.8	89	− 59	91	20.44	1.15	622.3		120	69
IPN70PE30PU	329.2	329.7	95	− 62	17	17.14	1.14	724.7		114	33^{b}
IPN60PE40PU	309.9	311.5	100	− 63	15	11.96	1.13	1042.1	30^{a}	116	25^{b}
IPN50PE50PU	289.1	293.4	97	− 64	17	7.99	1.11	1516.7	30^{a}	115	25
IPN40PE60PU	270.2	275.3	105	− 62	12	6.33	1.10	1914.9	32	113	25
IPN30PE70PU	257.0	257.1	112	− 64	9	5.02	1.09	2211.0	37	98^{a}	28
IPN20PE80PU	237.2	239.0	115	− 62	12	4.47	1.08	2350.7	37	84^{a}	26
IPN10PE90PU	220.3	220.8	117	− 59	13	3.86	1.07	2499.9	39		28
IPN0PE100PU	202.7	202.7	125	− 61	19	3.61	1.06	2667.4	41		31

[b] These indicate a shoulder over 65°C.

[a] Weak peaks or shoulders on the main peak.

1.34, is the molar relationship between the styrene and polyester double bonds.

3. Results and discussion

Fig. 1 shows the DSC thermographs of the dynamic curing of the various IPNs. It can be seen that the IPNs are completely miscible before reacting and show a single T_{go} that appears at a practically constant temperature (Table 1). Analysis of the peak curing temperature T_{p} (Fig. 1 and Table 1) shows that the curing kinetics is modified for all the IPN formulations and thus accelerates the reactive process with respect to that which exists in pure homopolymers. In Table 1, the experimental reaction heats (Δh_{dyn}) are shown and compared with theoretical predictions. From the experimental reaction heat of pure polyester and polyurethane, reaction heats for each reactive group of 65.4 J/mol C=C and 70.2 J/mol N=C=O were estimated. These values agree with those tabulated in the literature for equivalent reactive systems [23–25]. Taking these data into account, together with the formulation of each IPN, the theoretical reaction heats associated with the complete conversion of all the reactive groups were obtained. Agreement between the experimental and theoretical heats together with the absence of residual heat indicates that the IPNs formed reacted completely. It is thus expected that high-property full IPNs with an associated thermoset behaviour are produced.

Fig. 2 shows the evolution over time of the FTIR spectrum of IPN70PE30PU cured at 60°C. The decrease of the carbonyl band at 1728 cm^{-1} as the reaction progresses when pure polyurethane increased slightly and pure polyester remained the same, is indicative of collateral reactions between the isocyanate groups and the COOH and OH polyester terminal groups. This means that the IPNs formed possess chemical bonds between the two networks (graft-IPNs) and thus a high degree of intermixing. The decrease of the absorbance of the 2274, 1645 and 1630 cm^{-1} bands

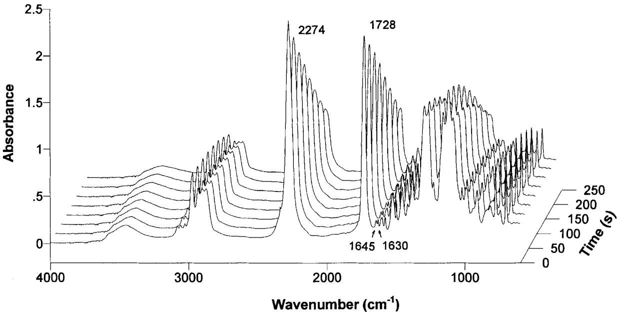

Fig. 2. FTIR spectra of IPN70PE30PU reaction at 60°C.

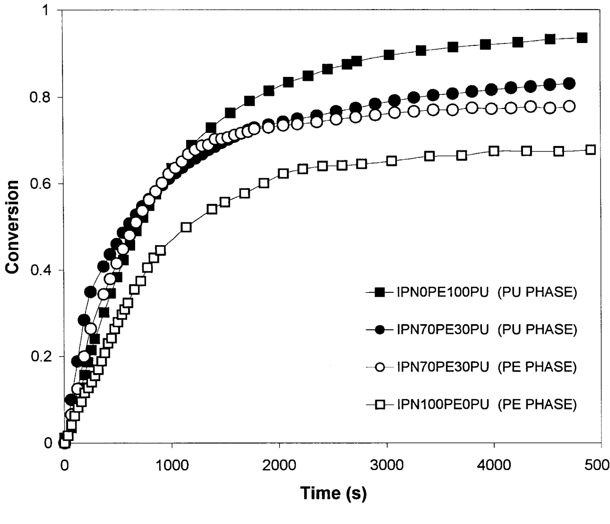

Fig. 3. Conversion versus time for IPN70PE30PU, IPN100PE0PU and IPN0PE100PU reactions, measured by FTIR at 60°C.

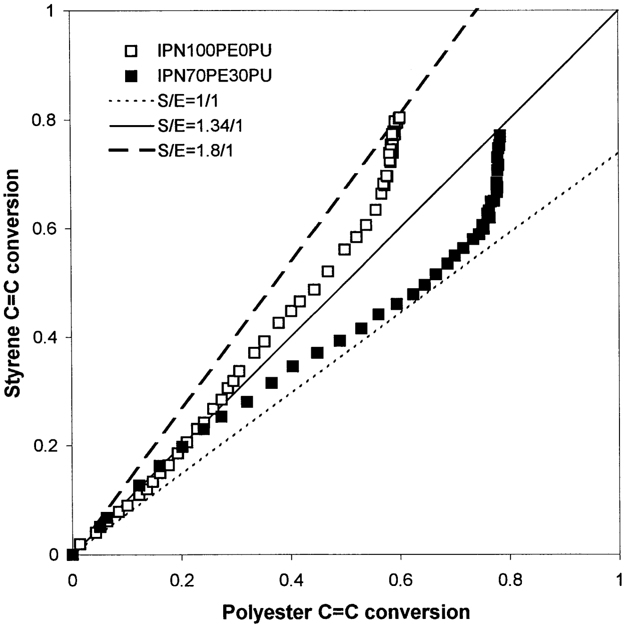

Fig. 4. Styrene C=C conversion versus polyester C=C conversion for IPN100PE0PU and IPN70PE30PU reactions at 60°C.

allowed evaluation of the polyurethane and polyester phase conversion. In Fig. 3, the polyurethane and polyester phase conversions in the IPN70PE30PU cured at 60°C are shown and compared with the conversions of pure polyurethane and polyester. It can be seen that both thermoset components react simultaneously, although at different rates. It can also be seen in Fig. 3 that both in the polyurethane phase, with a conversion of 60%, and in the polyester phase, throughout the range studied, that the reaction takes place at a higher rate than in the pure components. The consumption acceleration of the isocyanate groups in the IPN may be explained by the collateral reactions between the isocyanate groups and the carbonyl groups and terminal hydroxyls of the unsaturated polyester and by a certain solvent effect of PE on PU due. The increase in the reaction rate of the unsaturated polyester resin in the IPN may be explained by the fact that the polyurethane phase is much less crosslinked than the polyester phase is. The radicals that propagate in the polyester–polyurethane mixed medium thus encounter fewer physical barriers than when there is only polyester resin. Conversions of the isocyanate, styrene and polyester groups were complete in all of the IPNs after 24 h at 60°C with postcuring of 1 h at 180°C. This result contradicts the fact that during the curing process, the pure polyester resin always remains near 10% of the unsaturation values, which basically arise from the polyester ($\alpha_{\text{styrene}} = 95\text{–}98\%$ and $\alpha_{\text{polyester}} = 80\text{–}85\%$), which do not react due to topological impediments [21,26]. As has been said for IPNs, the existence of a fraction of the polyurethane phase, of a lower crosslinking density, means that there are fewer impediments and that the C=C of the polyester react completely and at a higher rate than pure polyester.

The collateral reactions between the polyurethane isocyanate groups and the terminal unsaturated polyester COOH may lead to the formation of amines according to the following scheme:

$$\text{R–N=C=O} + \text{R}'\text{–COOH} \rightarrow \text{R–NH–CO–O–OC–R}'$$

$$\rightarrow \text{R–NH–CO–R}' + \text{CO}_2$$

These amines may act as promoters of the curing process (redox initiation by decomposition of MEKP) by increasing the reaction rate of the unsaturated polyester. The existence of water in the reaction medium would also lead to the formation of amines by reaction of water with the isocyanate groups.

In previous work [27,28] we determined, for the PE phase, the conversion to gelling close to 45% using thermomechanical analysis, DMTA and solubility tests. For the PU phase, a theoretical conversion to gelling of 76.7% was determined using the statistical theory of Flory [29]:

$$\alpha_{\text{gel}} = \left[\frac{1}{(f_{\text{P}} - 1)(f_{\text{I}} - 1)} \right]^{1/2} \tag{3}$$

α_{gel} is the conversion to gelling, and f_{P} and f_{I} are the functionality of polyol and isocyanate, which for polyurethane in this study are 2 and 2.7 respectively. The values of α_{gel} of the PU and PE phases justify the results obtained by FTIR (Fig. 3). It can be seen, as in the case of the IPNs, that the PE phase gels before the PU phase. Thus, while the PE did not gelled the PU reacted at a higher rate than polyester and the pure polyurethane, from this instant this tendency changes and the PU reaction rate decreases. This is due to the fact that the PE phase possesses a greater crosslinking density and in this medium, the PU reacts more slowly and reaches a final conversion substantially lower than that of pure polyurethane.

In PU/PE IPNs, several authors [24] have detected a contrary effect to what has been observed in this study. They have seen that when the PU content is increased, the PE reaction takes place in longer time period at a lower rate and the final conversion decreases. This apparent contradiction may be explained, in their case, by the fact that the PU phase gels and reaches almost complete conversion before the PE phase starts reacting. These results show the important role that the relative gelling of the two phases plays in the polymerization rates and consequently in the morphology of the IPNs.

During curing of unsaturated polyester, the chains may crosslink with or without styrene, intermolecularly and intramolecularly. The intermolecular reactions lead to the formation of the network through the connection between adjacent polyester chains, while the intramolecular connections increase their crosslinking density and reduce the size of the polyester coils, but do not contribute to the forming of the network. Different morphologies may be formed depending on the relative amount of intermolecular and intramolecular crosslinks. The latter contributes to the

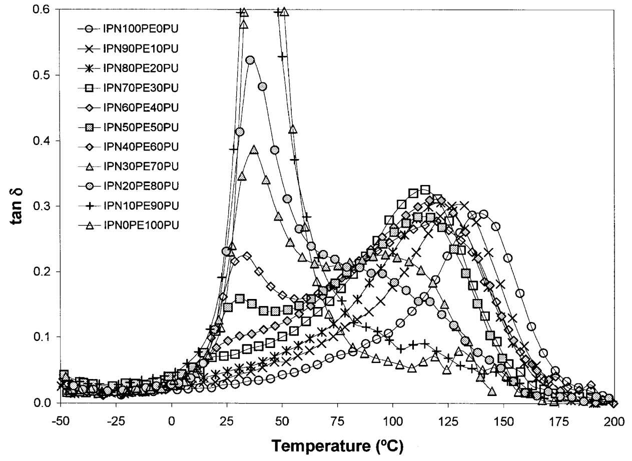

Fig. 5. Loss factor versus temperature for the polyurethane–polyester IPNs.

formation of microgels, whose size and structure depend on the formula used and the reaction mechanism [30].

Knowledge of the conversion of styrene as opposed to polyester in the polyester phase is important as the structure of the network in this phase strongly depends on the styrene–polyester copolymerization process. Fig. 4 shows this information for IPN70PE30PU and for pure polyester. Lines show the conversion when styrene and polyester react in different proportions (S/E). S/E is the ratio between the double bonds of styrene and polyester that react during curing. $S/E = 1/1$ corresponds to alternating copolymerization where each C=C of the styrene reacts with a C=C of the polyester. $S/E = 1.34/1$ represents azeotropic polymerization where styrene and polyester always react in the same proportion that existed at the beginning of the curing process. $S/E = 1.8/1$ refers to an azeotropic copolymerization calculated using reactivity ratios at 60°C of the copolymerization between diethyl fumarate and styrene [31–33]. The curing of pure polyester takes place between the $S/E = 1.8/1$ and $S/E = 1.34/1$ lines, which indicates a chemical control of the reactive process. Only at high conversions (higher than 50% polyester) is the $S/E = 1.8/1$ line passed and the reaction becomes controlled completely by diffusion. The same occurs in IPN70PE30PU from $\alpha_{\text{polyester}} = 0.75$. In both cases, the reaction of the styrene at high conversions (low concentration of C=C), is favoured more than that of the polyester. This is due to the fact that the polyester molecules are much more immobile than those of styrene as they form part of a crosslinked network. It can be seen that curing is not affected by the existence of PU in the IPN for conversion up to 30%. At this point, a greater amount of polyester in the IPN reacts and the process tends to alternate copolymerization. This behaviour is appreciably different to that seen in pure PE. A possible explanation is that the PU phase favours intramolecular interactions of the polyester molecules. In Fig. 4, it can also be seen that beyond 30% conversion, at the same polyester conversion, more styrene has been consumed in the pure PE than in the IPN due to the strong interaction of the PU phase. This changes the styrene–polyester copolymerization mechanism and consequently the morphology of the polyester phase.

The morphology and miscibility of IPNs can be studied by DMTA. The graph of the storage module, E', at a given temperature versus the composition may be related to models that predict phase continuity and phase inversion in polymer blends. In the graph of tan δ versus temperature, a narrow peak of the loss factor indicates a high degree of miscibility, while the two clearly separated transitions with a low value of tan δ in the inter-transition indicate large phase separation. The intermediate situation for semi-miscible IPNs is represented by a single broad transition. Two peaks of tan δ of the same height may be indicative of two continuous phases or phase inversion [13,34].

Fig. 5 shows the curves of tan δ versus temperature for synthesized IPNs. The relaxation associated with the glass transition can be seen. Although all the samples are transparent, for some intermediate formulations, especially IPN60PE40PU, IPN50PE50PU and IPN40PE60PU, the existence of two domains is evident, which can be attributed to separate polyurethane and polyester phases. Formulations that are rich in one component show a single domain. IPNs with a composition close to that of pure PE show a wide transition due to the fact that pure PE has a wide relaxation spectrum. The dynamical mechanical relaxations (maximum of tan δ) labelled T_1 and T_2 in an increasing order of temperature are shown in Table 1. The polyurethane phase shows a transition, T_1, at a lower temperature than the polyester phase, T_2, due to the fact that it possesses greater mobility and a less crosslinked network. In formulations that are rich in PU, T_1 is only slightly affected by PE. However, when the majority component is PE, T_2 decreases by a plasticization effect of the PU on the PE. The existence of T_1s that are slightly less than that of pure PU, in formulations that are rich in PU, may be explained by physical effects, such as the loosened molecular packing, the plasticization or the incomplete formation of the PU network

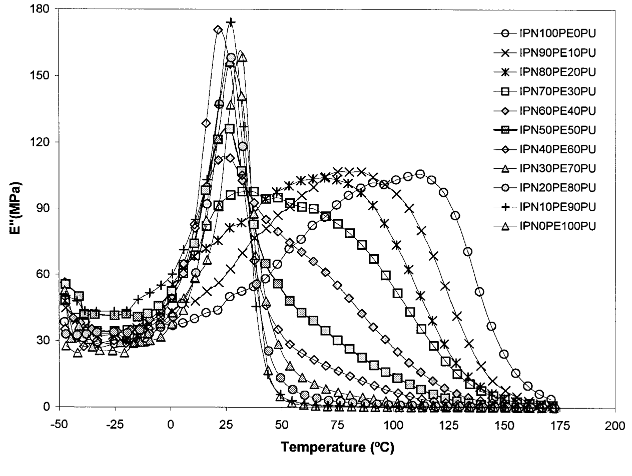

Fig. 6. Loss modulus versus temperature for the polyurethane–polyester IPNs.

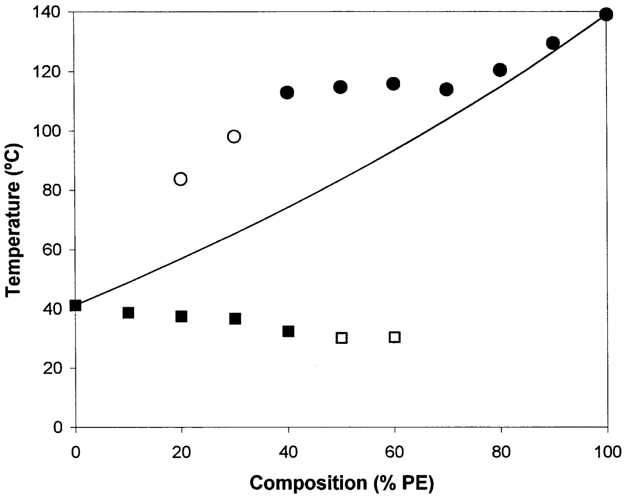

Fig. 7. Relaxation temperatures, at 1 Hz, (based on tan δ peak temperatures) versus composition. (●) T_2 principal relaxation, (○) T_2 shoulder or weak peak, (■) T_1 principal relaxation, (□) T_1 shoulder or weak peak. The line represents the prediction of the Fox equation.

containing defects. The fact that in the (IPN60PE40PU, IPN50PE50PU and IPN40PE60PU) formulations, T_2 are less than the value of the pure PE, is indicative that there is a certain miscibility in mid-range compositions.

Fig. 6 shows the loss modulus, E'', versus the temperature for the studied IPNs. Table 1 contains the peak temperature of E'', $T_{E''}$, associated with the relaxation of the glass transition. In general, a single transition is seen and only some intermediate compositions present a shoulder.

The values of the calorimetric T_g with those of T_1 and T_2 are compared in Table 1. It can be seen that a glass transition is detected by DSC, which seems to indicate that there is no phase separation. A closer analysis by DMTA shows the existence of two domains in some formulations, which are not detected by DSC. The fact that only one $T_{E''}$ and one calorimetric T_g are detected, while the two maximums in tan δ are related to the fact that polyurethane possesses E'' values in the maximum and the change in heat capacity at the glass transition $\Delta c_p(T_g)$ is much greater than polyester ($E''_{\max PU} = 165$ MPa, $E''_{\max PE} = 105$ MPa, $\Delta c_p(T_g)_{PU} = 0.41$ J/g K, $\Delta c_p(T_g)_{PE} = 0.19$ J/g K). Therefore, certain domains in the PE phase are not seen in E'', nor in the calorimetric glass transition, but they are seen in tan δ and in the E'–T curve (Fig. 8).

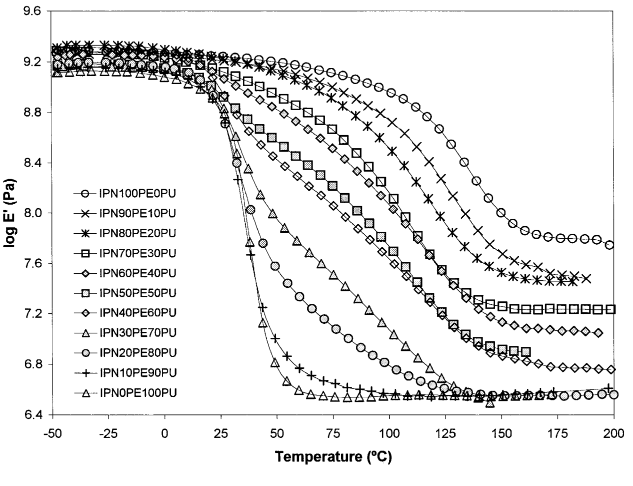

Fig. 8. Storage modulus versus temperature for the polyurethane–polyester IPNs.

Fig. 7 shows graphs of the T_1, T_2 transitions versus composition, together with the prediction of the Fox equation [35]:

$$\frac{1}{T_g} = \frac{W_1}{T_{g1}} + \frac{W_2}{T_{g2}} \tag{4}$$

where the subscripts 1 and 2 refer to the two polymers, W is the mass fraction and T the temperature in absolute units. Only for 90, 80 and 70% in polyester do the empirical data match the Fox equation. Intermediate compositions, as expected, did not fit the prediction as the transitions were asymmetric and in some cases were double or displayed a shoulder. Equivalent results are obtained using a mixture relationship of the type: $T_g = W_1T_{g1} + W_2T_{g2}$.

Fig. 8 shows the curves of log E' versus temperature for synthesized IPNs. It can be seen from the figure that the IPN*x*PE*y*PUs present a semi-miscible morphology. The storage module does not decrease suddenly in two stages, which would indicate the existence of two phases. It can also be seen there is a strong influence of composition on the elastic modulus. When the polyurethane content increases, the rigidity of the system decreases. In Table 1, the equilibrium rubber elastic modulus, E_r, of the IPNs is shown, estimated at the temperature of the peak of tan δ plus 50°C. The crosslinking density was determined from the number-average molecular weight between crosslinked junctions, M_c. The estimation of M_c was done from simple rubber elasticity theory considering the front factor to be unity and using [36–39]:

$$M_c = \frac{3dRT}{E_r} \tag{5}$$

where d is the density of the material, T the Kelvin temperature and R the universal gas constant. When polyurethane content is increased, both the crosslinking density (M_c increases) and the E_r modulus decrease (Table 1). While the PU phase has very few crosslinks and is very flexible, the PE phase shows a high degree of crosslinking and is very rigid. The synthesized IPNs show an intermediate stage between these two extremes as a function of composition. This fact is indicative of a high degree of interpenetration.

For comparison with simultaneous IPNs, sequential IPN40PE60PU has been prepared by changing the initiation system MEKP/CoOc for 2% benzoil peroxide. In this way, the PE reacts when all of the PU has crosslinked. In Fig. 9, the results of the DMTA analysis for sequential and simultaneous IPN40PE60PU are shown. It can be seen, in the curves of tan δ–T and E'–T, that the sequential IPN

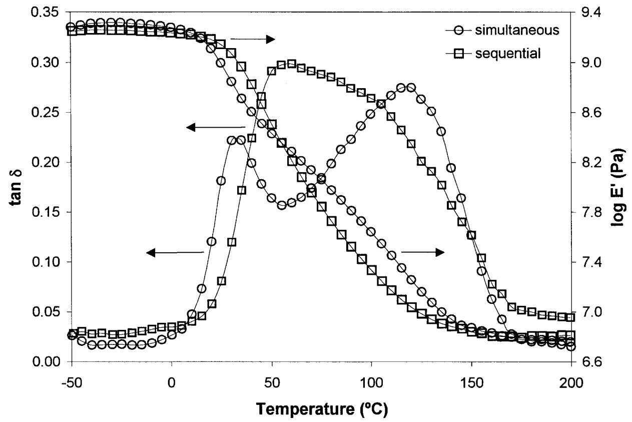

Fig. 9. Dynamical mechanical properties for IPN40PE60PU sequential and simultaneous.

shows a lower tendency to phase separation than the simultaneous IPN, in contrast with what is seen in other IPN families [19,40]. In the sequential IPN, a continuous fall in the modulus and a single broad transition is seen, whose temperature follows the Fox equation. The sequential IPN may yield a lower phase separation, as when it starts to react the PE, and PU phase has gelled and furthermore the graft reactions between networks have been completed. The free space remaining for the PE phase to separate is, therefore, small. In the case of simultaneous IPNs (Fig. 3), the PE gels first ($\alpha_{\mathrm{gel,PE}} = 45\%$), as it possesses a greater crosslinking density; before gelling and the termination of the graft reactions, the PU has reacted extensively ($\alpha_{\mathrm{PU}} \approx 50\%$), and domains of some size may form. It can be concluded that the phase separation in IPNs does not depend on whether these are sequential or simultaneous, but on which polymer gels first, the conversion reached by the polymers when the first gels and the existence or otherwise of graft polymerizations. In general, if the conversion of both polymers is high before one of them gels, greater phase separation can be expected.

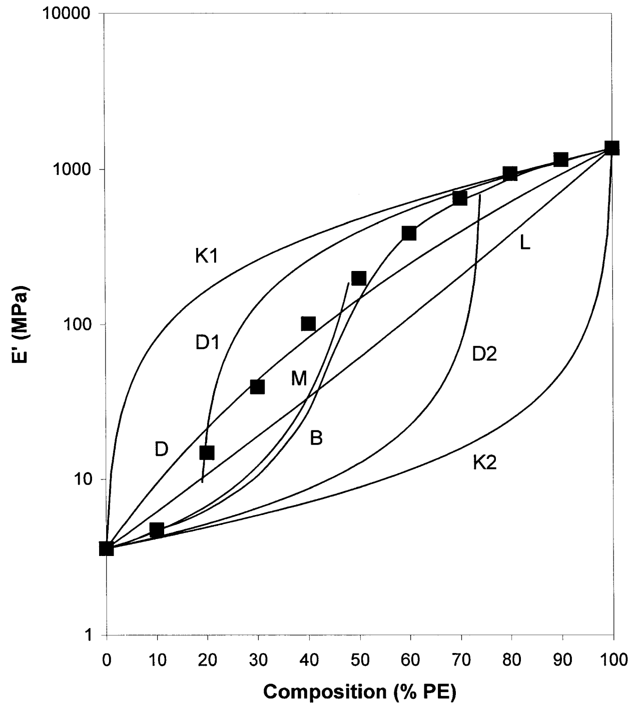

Fig. 10. Storage modulus versus composition data for the polyurethane–polyester IPNs compared with modulus–composition models at 70°C and 1 Hz. (■) the experimental data; M the Mooney equation Eq. (6); K1 and K2 the upper and lower bounds of the Kerner equation Eq. (7); D1 and D2 the upper and lower bounds of de Dickie equation Eq. (9); D the Davies equation Eq. (11); B the Budiansky equation Eq. (12); L the logarithmic rule of mixing.

The modulus–composition relationship has been analysed for the synthesized IPNs using theoretical equations based on mechanical models. Most of these models assume perfect adhesion between the homogenous isotropic phases and that inclusions in the matrix are spherical. Mooney [41] deduced, for elastomers with a Poisson ratio of 0.5, filled with spherical particles:

$$E = \frac{(1+\nu)}{(1+\nu_{\mathrm{m}})} E_{\mathrm{m}} \exp\left(\frac{2.5 V_{\mathrm{i}} \phi_{\mathrm{m}}}{\phi_{\mathrm{m}} - V_{\mathrm{i}}}\right) \tag{6}$$

where E and E_{m} are the tensile modulus of the composite and the matrix, ν and ν_{m} are the Poisson's ratios of the composite and the matrix, V_{i} is the fraction in volume of inclusion and ϕ_{m} is the maximum fraction of packing for rigid inclusions in a elastomeric matrix.

Kerner [42] developed a model for matrices with spherical inclusions, which in tensile modulus terms can be written as [11]:

$$\frac{E}{E_{\mathrm{m}}} = \frac{\gamma(1 - V_{\mathrm{i}})E_{\mathrm{m}} + \beta(\alpha + V_{\mathrm{i}})E_{\mathrm{i}}}{(1 + \alpha V_{\mathrm{i}})E_{\mathrm{m}} + \alpha\beta(1 - V_{\mathrm{i}})E_{\mathrm{i}}} \tag{7}$$

where

$$\alpha = \frac{2(4 - 5\nu_{\mathrm{m}})}{(7 - 5\nu_{\mathrm{m}})},\ \beta = \frac{(1 + \nu_{\mathrm{m}})}{(1 + \nu_{\mathrm{i}})},\ \gamma = \frac{(1 + \nu)}{(1 + \nu_{\mathrm{m}})} \tag{8}$$

The subscript m indicates a matrix and i an inclusion.

Dickie [43] modified Kerner's equation and introduced the ψ parameter to take into account the maximum fraction of volume that may be occupied by the disperse particle phase:

$$\frac{E}{E_{\mathrm{m}}} = \frac{\gamma(1 - \psi V_{\mathrm{i}})E_{\mathrm{m}} + \beta(\alpha + \psi V_{\mathrm{i}})E_{\mathrm{i}}}{(1 + \alpha\psi V_{\mathrm{i}})E_{\mathrm{m}} + \alpha\beta(1 - \psi V_{\mathrm{i}})E_{\mathrm{i}}} \tag{9}$$

where

$$\psi = 1 + \frac{V_{\mathrm{i}}(1 - \phi_{\mathrm{m}})}{\phi_{\mathrm{m}}^2} \tag{10}$$

All these models predict the properties of the composites better if the fraction in the disperse phase volume is small, as it supposes that there are no interactions between the different domains of this phase.

Davis [44] proposed the following relationship for systems in which both components are present as continuous

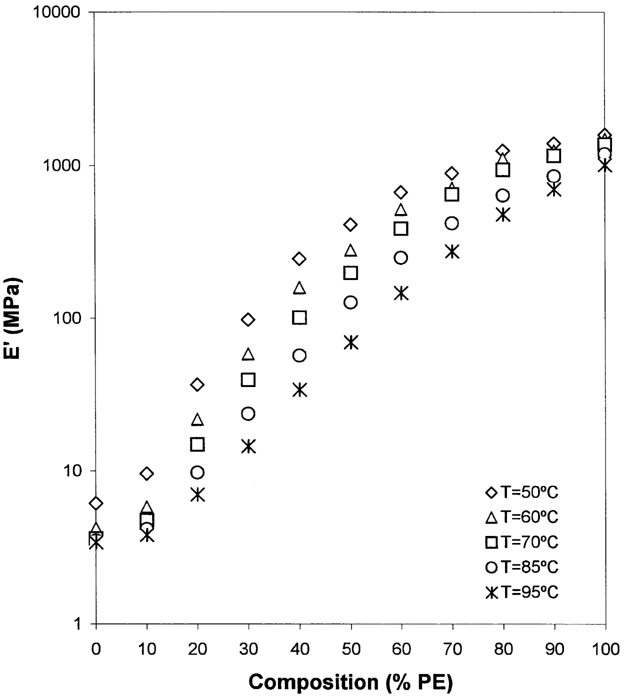

Fig. 11. Storage modulus versus composition data at different temperatures.

phases (dual-phase continuity):

$$G^{1/5} = \phi_1 G_1^{1/5} + \phi_2 G_2^{1/5} \tag{11}$$

where G is the shear modulus, ϕ the fraction in volume and the subscripts 1 and 2 represent the components of the IPN or the blend.

Budiansky [45] developed a model that predicts the phase inversion in the mid composition range:

$$\frac{\phi_1}{1+\epsilon\left(\frac{G_1}{G-1}\right)} + \frac{\phi_2}{1+\epsilon\left(\frac{G_2}{G-1}\right)} = 1 \tag{12}$$

G, ϕ and the subscripts mean the same as in eq. (11). ϵ is related to Poisson's ratio, ν, through the following equation:

$$\epsilon = \frac{2(4-5\nu)}{15(1-\nu)} \tag{13}$$

The five modulus–composition theories described were used in terms of the storage modulus to study phase continuity in the synthesized IPNs. For the homopolymers Poisson's ratios were taken, $\nu = 0.5$ for polyurethane and $\nu = 0.37$ for polyester [46]. The Poisson's ratios for the IPNs were calculated using a linear rule of mixture of volumes [11,42]. The shear modulus, G, and the tensile modulus, E, were converted using the relationship $E = 2G(1+\nu)$. For rigid inclusions in an elastomer matrix, the maximum packing fraction was chosen, $\phi_m = 0.64$, while for the elastomer inclusions in a rigid matrix $\phi_m = 0.83$ [11]. Fig. 10 shows the empirical storage modulus (1 Hz) versus composition of the IPN at 70°C and the curves obtained from Eqs. (6),(7),(9),(11) and (12). Although the experimental points do not fit any model exactly, it can be seen that the Budiansky equation, which involves phase inversion in the intermediate compositions, is the best approximation. The form of the Budiansky equation and the experimental data is similar, but in the latter, the phase inversion has shifted to a composition near 30% in PE. At low compositions in PE, there is a continuous matrix of dominant polyurethane, and subsequently there are other compositions in which there is a co-continuous structure (phase inversion) with two continuous phases and finally for compositions rich in PE, the PE becomes the dominant continuous phase. As the PU phase is in a rubbery state and the PE phase in a glassy state, the E'-composition (%) may be understood as a glass transition at constant temperature, where the material changes from being glassy to rubbery as the composition changes. In the literature, it can be seen how the results of fitting the experimental data to modulus–composition theories are contradictory, when comparing static and dynamic properties (i.e. elastic modulus and dynamic storage modulus) [11,12]. As explained by Hourston and Schäfer [13], this is due to the effect of the temperature selected for the study and the frequency used, which in dynamic experiments is equivalent to temperature. To establish this effect, Fig. 11 shows the experimental modulus–composition curves at different temperatures. It can be seen that the phase inversion shifts as a function of the chosen temperature. When the temperature is closer to the transition of the component that has the lowest T_g, the phase inversion appears at richer compositions in this component. The arbitrary choice of temperature does not take into account the different expansion coefficients of the two components and that the properties of these components

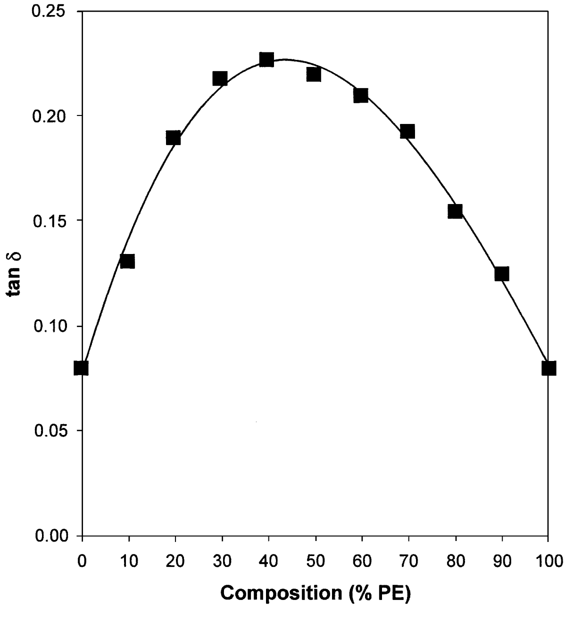

Fig. 12. Loss factor (values taken at 85°C) versus composition.

in IPNs are not exactly the same as in the homopolymers [13,47]. To eliminate the effect of temperature, a working temperature of 85°C was chosen by applying two criteria. Firstly, because this temperature is the mid-point between the temperature of the inflexion point of the $E'-T$ curves of the pure homopolymers [13]. The second criterion is that the two pure components should have the same value of tan δ [47]. In our case, the two criteria practically give the same temperature. It can be seen (Fig. 11) that at 85°C, phase inversion seems to take place near 40% in PE. This result is coherent for this composition as two peaks of a similar height appear in the tan $\delta-T$ curve (Fig. 5). If the study is required to be carried out at room temperature to compare the dynamic results with static ones, a polyurethane showing a lower degree of crosslinking should be used.

Mechanical properties associated with molecular relaxation and energy dissipation are closely related to tan δ [12]. For example, there must exist a clear relationship between percentage elongation at failure or the toughness index and the loss factor. Although static mechanical tests were not performed, Fig. 12 shows the curve of tan δ versus composition at a temperature of 85°C. It can be seen that there is strong synergism and the properties of the optimum IPN greatly surpass those of the homopolymers. The optimum properties were shown for IPN40PE60PU, which is the formulation that has the greatest capacity to absorb energy. This result is coherent with a high degree of interpenetration.

4. Conclusions

The IPNs are completely miscible before reacting and once they are synthesized possess a high degree of conversion, which means high chemical stability and overall thermoset behaviour.

Using FTIR spectrophotometer, we have been able to prove that the synthesized IPNs are simultaneous and that the curing kinetics of polyester and polyurethane are modified significantly during the formation of the IPNs (PE and PU react at a higher rate in the IPNs than in pure homopolymers) due to the different mobility of the medium and the existence of collateral reactions. Changes in the styrene–polyester copolymerization mechanism have been detected. While in pure polyester an azeotropic polymerization takes place and the conversion is never complete, in the IPNs the copolymerization tends to be alternating and total conversion is reached in all of the reactive groups. The modification of the copolymerization mechanism also affects the change of chemical control to control by diffusion and appears in IPNs at polyester conversions higher than in pure polyester.

The crosslinking density of the phase that gels first, the conversion reached when this gelling occurs and the existence of graft reactions are determining factors in the morphology of an IPN formed in this way, together with the existence or otherwise of phase separation. Specifically, the sequential IPNs show a lower tendency to phase separation than the simultaneous IPNs, as when the polyester phase begins to react both the curing of the polyurethane phase and the graft reactions have been completed.

From a physical point of view, the results obtained with DMTA clearly show that there is a considerable variation of the elastic modulus and the crosslinking density in function of the proportion used and, therefore, the goal of reducing the rigidity of the polyester, or improving the poor properties of the polyurethane, is achieved.

The analysis of the relaxation associated with the glass transition proves that the synthesized IPNs show semi-miscible behaviour and in some intermediate formulations, there are two clear domains which can be attributed to separate polyurethane and polyester crosslinking. Between the peaks that characterize these relaxations, there is an area of overlap whose scope and size varies as a function of the proportion of the components used.

The modulus–composition curve follows the Budiansky equation, which predicts phase inversion in the range of intermediate compositions. Specifically, three different morphologies with phase inversion near IPN40PE60PU have been obtained. Compositions that are rich in PU show a continuous PU matrix with disperse PE, while formulations that are rich in PE show the opposite. Intermediate compositions show signs of the existence of two co-continuous phases.

If the relationship between the modulus and the composition is studied, the temperature at which the modulus is chosen strongly affects the shape of the modulus–composition curve. To avoid this influence, modulus–composition studies should be carried out at an intermediate temperature between the inflexion points of the storage modulus of the pure components or at a temperature where the loss factor has the same value for both homopolymers. With these criteria, phase inversion takes place for IPN40PE60PU, which agrees with other results obtained.

Strong synergism has been found in the loss factor, which indicates a high degree of interpenetration. Maximum properties appear close to IPN40PE60PU.

Acknowledgements

The research was supported by CICYT under Grant No. MAT2000-1002-C02-02.

References

[1] Manson JA, Sperling LH. Polymer blends and composites. New York: Plenum, 1976. Chapter 8.

[2] Klempner D, Berkowsky L. In: Mark H, Bikales NM, Verberger CGO, Menges G, editors. Encyclopedia of polymer science and engineering, Vol. 8. New York: Wiley, 1988.

[3] Hourston DJ, Song M, Shafer FU, Pollock HM, Hammiche A. Thermochim Acta 1998;324:109.

[4] Jo WH, Song JM, Ko MB. J Polym Sci: Part B: Polym Phys 2000;38:1005.
[5] Tomas DA, Sperling LH. In: Paul DR, Newman S, editors. Polymer blends, Vol. 2. New York: Academic Press, 1988 Chapter 11.
[6] Olabisi O, Robeson LM, Shaw MT. Polymer–polymer miscibility. New York: Academic Press, 1979.
[7] Kaplan DS. J Appl Polym Sci 1976;20:2615.
[8] Frisch K, Klempner D, Mignal S. J Polym Sci, Polym Chem Ed 1974;12:885.
[9] Kim SC, Klempner D, Frisch KC, Radigan W, Frisch HL. Macromolecules 1976;9:258.
[10] Sperling L. Polym Engng Sci 1985;25:517.
[11] Kim SC, Klempner D, Frisch KC, Frisch HL. Macromolecules 1977;10:1187.
[12] Akay M, Rollins SN. Polymer 1993;35:1865.
[13] Hourston DJ, Schäfer FU. Polymer 1996;37:3521.
[14] Wilkinson TC, Borgnaes D, Chappell SF, Kelly WL. Polym Prepr (Am Chem Soc, Mater Sci Engng) 1983;49:496.
[15] Kim JH, Kim SC. Polym Engng Sci 1987;27:1252.
[16] Yang YS, Lee LJ. Macromolecules 1987;20:1490.
[17] Chou YC, Lee LJ. Polym Engng Sci 1995;35:976.
[18] Fan LH, Hu CP, Pan CQ, Zhang CP, Yink SK. Polymer 1997;38:3609.
[19] Hua FJ, Hu CP. Eur Polym J 1999;35:103.
[20] Urban MW, Gabury SR, Provder T. Polymer 1991;32:171.
[21] Ramis X, Salla JM. J Polym Sci: Part B: Polym Phys 1999;37:751.
[22] Xue SC, Zhang ZP, Ying SK. Polymer 1989;30:1269.
[23] Ramis X, Salla JM. J Appl Polym Sci 1992;45:227.
[24] Hsu TJ, Lee LJ. Polym Engng Sci 1985;25:951.
[25] Lucas JC, Borrajo J, Williams RJJ. Poymer 1993;34:3216.
[26] Huang YJ, Chen CJ. J Appl Polym Sci 1992;46:1573.
[27] Cadenato A, Salla JM, Ramis X, Morancho JM, Marroyo LM, Martin JL. J Therm Anal 1997;49:269.
[28] Ramis X, Salla JM. J Polym Sci: Part B: Polym Phys 1997;35:371.
[29] Flory PJ. Principles of polymer chemistry. Ithaca, NY: Cornell University Press, 1953.
[30] Yang YS, Lee LJ. Polymer 1988;29:1793.
[31] Lewis FM, Walling C, Cummings W, Mayo FR, Briggs ER. J Am Chem Soc 1947;70:1519.
[32] Funke W, Ködler S, Feinauer R. Macromol Chem 1961;49:52.
[33] Bermark P, Flodin P. Polymer 1987;28:1662.
[34] Sperling LH. Interpenetrating polymer networks and related materials. New York: Plenum Press, 1981.
[35] Fox TG. Bull Am Phys Soc 1956;1:123.
[36] Tobolsky AV, Carlson DW, Indictor N. J Polym Sci 1960;54:175.
[37] Nielsen LE. J Macromol Sci Macromol Chem 1969;C3(1):69.
[38] Vratsanos MS, Farris RJ. Polym Engng Sci 1989;29:806.
[39] De la Caba K, Guerrero P, Eceiza A, Mondragon I. Polymer 1996;37:275.
[40] Zhou P, Frisch HL. Macromolecules 1994;27:1788.
[41] Mooney MJ. Colloid Sci 1951;6:162.
[42] Kerner EH. Proc Phys Soc 1956;B69:808.
[43] Dickie RA. J Appl Polym Sci 1973;17:45.
[44] Davies WEA. J Phys D 1971;4:318.
[45] Budiansky B. J Mech Phys Solids 1965;13:223.
[46] Johnson AF. Engineering design properties of GRP. London: British Plastics Federation, 1979.
[47] Dickie RA. In: Paul DR, Newman S, editors. Polymer blends, Vol. 2. New York: Academic Press, 1988. Chapter 8.